Soldagem & Inspeção. 2017;22(2):194-206
http://dx.doi.org/10.1590/0104-9224/SI2202.08

Correlation of Stress Concentration Factors for T-Welded Connections – Finite Element Simulations and Fatigue Behavior

Gerardo Terán Méndez[1], Rubén Cuamatzi-Meléndez[2], Apolinar Albiter Hernández[2], Selene I. Capula-Colindres[1], Daniel Angeles-Herrera[2], Julio Cesar Velázquez[1], Omar Vazquez-Hernández[2]

[1] Instituto Politécnico Nacional, Departamento de Ingeniería Química Industrial – ESIQIE, Zacatenco, Ciudad de México, México.
[2] Instituto Mexicano del Petróleo, San Bartolo Atepehuacan, Ciudad de México, México.

Received: 20 Mar., 2017
Accepted: 5 July, 2017

E-mails: gerardoteranm@gmail.com (GTM), rcuamatzi@imp.mx (RCM), aalbiter@imp.mx (AAH), selenecapula@gmail.com (SICC), dangelesh0600@alumno.ipn.mx (DAH), jcva8008@yahoo.com.mx (JCV), ovazquez@imp.mx (OVH)

Abstract: The stress concentration factors (SCFs) in welded connections usually occur at zones with high stress levels. Stress concentrations reduce the fatigue behavior of welded connections in offshore structures and cracking can develop. By using the grinding technique, cracking can be eliminated. Stress concentration factors are defined as a ratio of maximum stress at the intersection to nominal stress on the brace. Defining the stress concentration factor is an important stage in the fatigue behavior of welded connections. Several approaches have evolved for designing structures with the classical S-N approach for estimating total life. This work correlates to the stress concentration factors of T-welded connections and the fatigue behavior. Stress concentration factors were computed with the finite element employing 3D T-welded connections with intact and grinding depth conditions. Then, T-welded connections were constructed with A36 plate steel and welded with E6013 electrodes to obtain the stress-life (S-N) approach. The methodology from previous works was used to compute the SCF and fabricate the T-welded connections. The results indicated that the grinding process could restore the fatigue life of the T-welded connections for SCFs values in the range of 1.29. This value can be considered to be a low SCF value in T-welded connection. However, for higher SCF values, the fatigue life decreased, compromising and reducing the structural integrity of the T-welded connections.

Keywords: Stress concentrations factors; Finite element method; T-welded connections; U-shape grinding; S-N curve.

1. Introduction

In the Gulf of Mexico, many offshore structures are operating in shallow water to process oil and gas, in aquatic depths of up to 120 meters. Platforms are built up, conforming to the following standards: NRF-003-PEMEX-2007 [1], NRF-175-PEMEX-2007 [2] and NRF-186-PEMEX-2007 [3]. Those standards recommend different steels (ASTM A36, A53 grade B, A572 grade 50, AP 2H grade 50, etc.) for tubular elements welded to each other, e.g. leg, bracing, caissons, etc. The structural elements are welded in different shapes, such as: T, K or K-T. Also, those welded connections are employed to reinforce different offshore structures.

In offshore structures, localized cracking can appear at the weld toe of the T-welded connections. Such structures operate under harsh environmental conditions, such as hurricanes, cyclones and storms, causing localized fatigue cracking. It is a real concern for the oil and gas industry [2,4], since the loads are dynamic. Cracking could be repaired by grinding the damaged regions [5]. Different repair techniques have been introduced to increase the fatigue life of offshore structures, such as burr grinding, tungsten inert gas (TIG) dressing, Hammer peening and Needle peening [6]. Those methods have been employed in ambient air and laboratory conditions and cannot be applied to eliminate localized cracking in underwater conditions. Their application is very difficult and expensive. Grinding can be used in underwater conditions, but the grinding process can affect the integrity of structural components when the grinding is performed without criteria.

Nowadays, fatigue work on T-welded connections has been carried out, repaired by U-shape grinding under plane stress condition [7-9]. A better approach was achieved by performing 3D finite element modelling and applying empirical formulations [8,10]. Unfortunately, the empirical formulations can only be applied for a U-shape grinding depth of 27% of the plate thickness. For example, in the industry, deep cracks can be identified at

up to 27% of the plate thickness. Therefore, it is necessary to evaluate higher grinding depths in order to eliminate higher amounts of damaged material and arrest crack propagation in T-welded connections. Consequently, it is essential to establish an appropriate U-shape grinding depth to repair the weld toe with localized damage [11,12] and to guarantee structural integrity [7,13].

In the present work, the SCFs obtained on T-welded connections were correlated with the classical S-N curves. The SCFs were estimated with finite element method modelling for both intact and grinding depth conditions. In this context, two U-shape grinding depths of 6 mm and 10 mm corresponding to 30% and 50% of the plate thickness, respectively, were proposed. U-shape grinding was selected by [8,10]. Also, the S-N curves were obtained for T-welded connections under bending load. T-welded connections were fabricated with ASTM A-36 plate steel and welded with E6013 electrodes.

2. Experimental Procedure

2.1. T-welded connections using finite element method

A lot of works have employed the finite element method for the analysis of the SCFs in Fixed Jacked Platforms [14-17], and welded connections [18-20] with reliable results. Under this frame of ideas, in these works, T-welded connections were selected to estimate SCFs through 3D finite element models. The methodology by [4] was used to compute the SCF and finite elements features were presented. Dimensions of T-welded connections are presented in Figure 1. Numerical models considered intact and repaired conditions appear in the same analysis. Due to the symmetry, U-shaped grinding is in the center of the T-welded connections, and it is possible to simulate only half of the T-welded connections, see Figure 2a). By applying symmetry in the Z-plane of the T-welded connections, half of the connections are used, see Figure 2b). Finite element models were subjected to bending loads [7, 21-25]. The load was applied to the Y-axis at a distance of 101.6 mm centered in the connection centerline. The model was restricted to the X and Y displacement in points A-A, and restricted to the Y direction from points B-B, see Figure 2c). SCFs were determined, conforming to the following Equation 1:

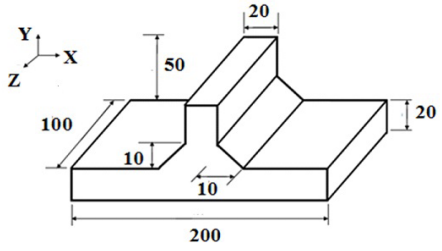

Figure 1. T-welded connections dimensions (unit: mm).

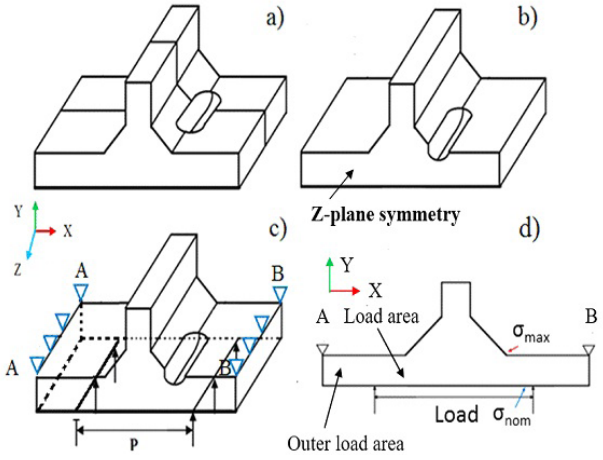

Figure 2. Scheme of the model. (a) U-shape grinding; (b) half of the T-welded connection with U-shape grinding; (c) load configuration and boundary conditions and; (d) $\sigma_{\max}$ and σ_{nom}.

$$SCF = \sigma_{\max} / \sigma_{nom} \quad (1)$$

where $\sigma_{\max}$ is the maximum stress at the weld toe and σ_{nom} is the nominal stress. The maximum stress was taken at the weld toe [26,27]. In this way, σ_{nom} was obtained from regions close to the weld toe, see Figure 2d). The maximum principal stresses were used in this work [22]. The finite element models were developed with the ANSYS commercial software [28].

For the finite element simulations, the following mechanical properties [4] of the A36 plates steel were applied: elastic modulus E=206 GPa; Poisson´s ratio ɣ=0.3 and yield stress (σ_y) = 250 MPa. To obtain reliable results it is important to conduct a calibration for the elements used [4]. The finite element size was calibrated and five different sizes were used to mesh the models in the range from 1 mm to 5 mm. The hexahedral element (solid 45 with 8 nodes) was adopted. A T-welded connection, under intact conditions, was selected to calibrate finite element size. The overview of T-welded connections meshed with element sizes of 1 mm, 3 mm and 5 mm is displayed in Figure 3.

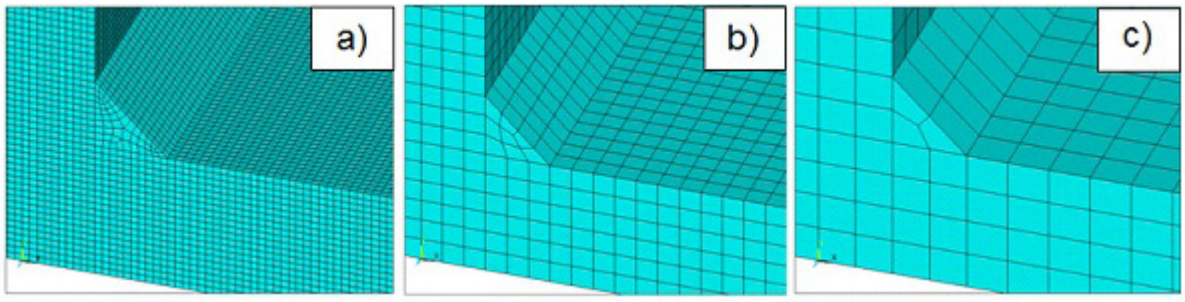

Figure 3. Elements size for 3D finite element models. (a) 1 mm; (b) 3 mm; and (c) 5 mm.

The finite element models were subjected to loads from 10% to 100% of the yield stress (σ_y), as shown in Figure 4. The SCFs values are consistent with stresses close to 250 MPa, but for higher stress levels, the SCFs dramatically reduced. This is because the material exceeds the yield stress and is situated in the plastic zone. Therefore, to obtain reliable results, in successive analysis, a load of 50% of the σ_y was chosen.

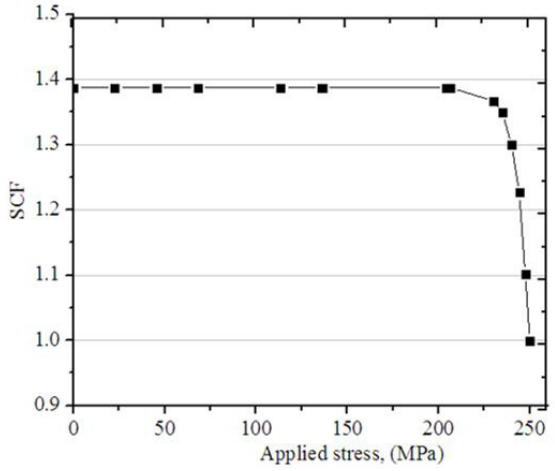

Figure 4. SCFs for different levels of stresses.

2.2. Fatigue testing of T-welded connections

Firstly, T-welded connections of A36 steel were fabricated, then, fatigue tests were developed. The connections were made with A36 plate steel with a thickness of 20 mm. The T-welded connections were welded employing E6013 electrodes following the procedure detailed by Terán et. al. [29,30] and according to the welding procedure

specification (WPS) AWS D.1.1/D1.1M code [31]. In those references [29,30] all variables are presented using the T-welded connections fabrication. Figure 5a) shows an intact T-welded connection. Figure 5b) presents the U-shape grinding at the weld toe. Critical regions of the welded connections, weld toe (W), edge of the grinding (E), and bottom of the grinding (B) are illustrated in Figure 5c). The U-shape grinding was carried out with a manual grinder machine employing a 4 mm diameter grinding wheel at 6000 rpm. The U-shape grinding geometry recommended by [8] could be used to eliminate localized cracking. Two different grinding depths of 6 mm and 10 mm, corresponding to 30% and 50% of the plate thickness respectively, were carried out at the weld toe of the T-welded connections.

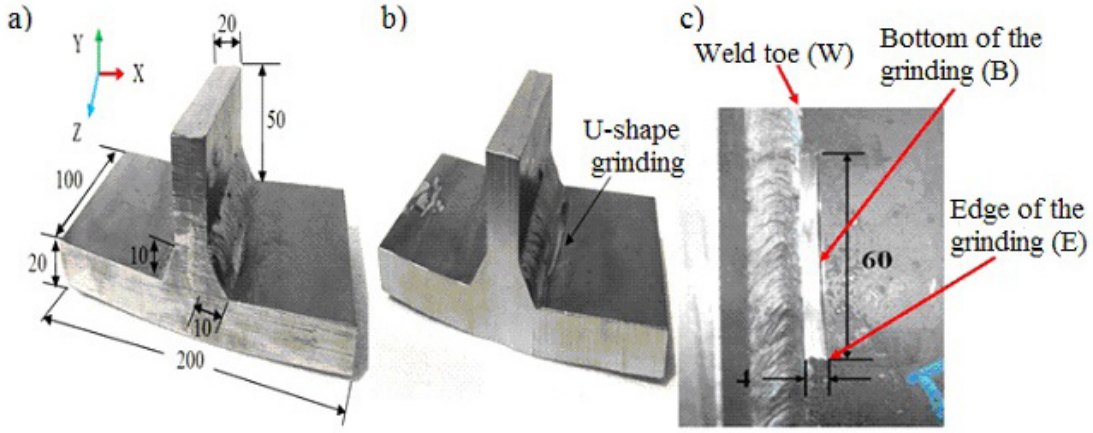

Figure 5. T-welded connection: (a) intact; (b) with U-shape grinding; and (c) critical regions of the U-shape grinding (units in mm).

The connections were welded at room temperature using the shielded metal arc welding (SMAW) process. All parameters in the welding process are presented in Table 1. The length of the T-welded connections is 100 mm for all specimens.

Table 1. Parameters in the welding process.

Number of weld beads	Electrode diameter (mm)	Current (A)	Voltage (V)	Polarity	Welding speed (mm/min)
1	3.2	80-120	28-32	DC (+)	254
2	3.2	80-120	28-32	DC (+)	355
3	2.4	60-90	28-32	DC (+)	203
4 or 5	4	110-160	28-32	DC (+)	254

T-welded connections were subjected to fatigue testing. Fatigue tests were conducted in a 10 ton MTS 810 servo, hydraulic testing machine, with a load frequency of 26.7 Hz, under a uniaxial load and with a stress ratio of R=0. The tests were performed at room temperature (23 °C) following the recommendations of ASTM E466 [32]. Values obtained are presented as stresses and fatigue life by a linear regression described by [33,34]. Figure 6 shows the experimental set up and the loading configuration. Table 2 presents the number of specimens tested and the testing conditions. The fatigue resistance evaluation recommended by IIW [35] includes fatigue resistance for non –load carrying fillet joints of 80 MPa, which is the characteristic fatigue strength at 2 million cycles, and a failure of 5% (FAT), with a constant inverse slope value of m=3. However, FAT evaluation is conservative and underestimates the fatigue life [24]. To obtain the S-N curve, T-welded connections were under loads that exceed the yield stress of the material (205 MPa). Furthermore, in the present work, a few T-welded connections were tested: 9 for intact T-welded connections, 4 for a grinding depth of 6 mm and 4 for a grinding depth of 10 mm.

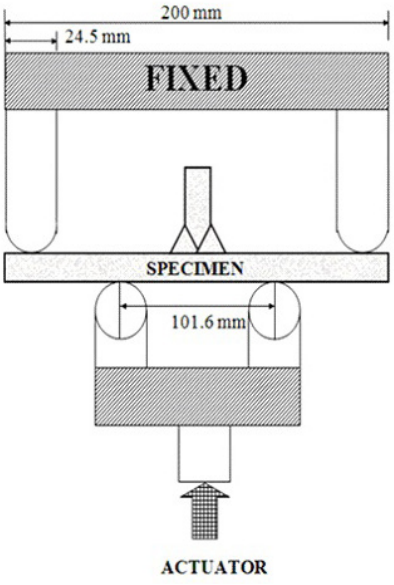

Figure 6. Load setup configuration for fatigue testing.

Table 2. T-welded connections for fatigue tests.

T-welded connections	Testing condition	Specimens No.
Intact	Room temperature	9
Grinding depth of 6 mm	Room temperature	4
Grinding depth of 10 mm	Room temperature	4

3. Results and Discussion

3.1. SCF´s obtained by finite element method

The SCFs obtained with the aforementioned procedure have been compared, as graphed in Figure 7. A small variation of the SCFs values for the different finite element size of 2 mm to 5 mm was observed. Also, the graph shows how the finite element size has a strong influence on the SCFs data. The results are coherent with little

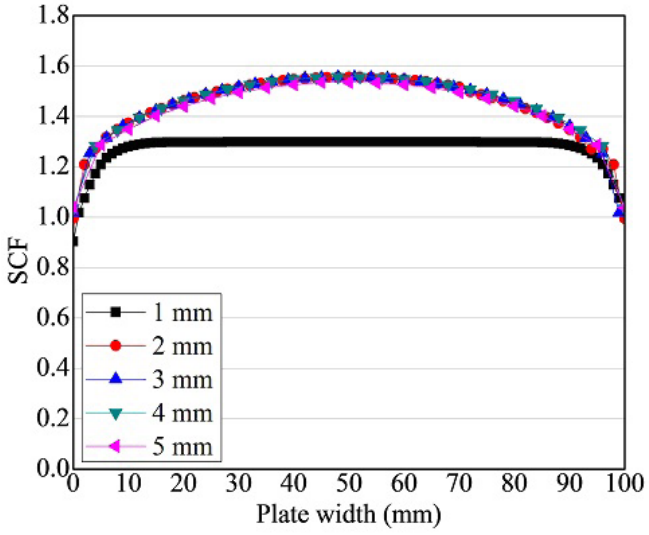

Figure 7. Finite element size effect on an intact T-welded connection.

variation in finite element size between 2 mm to 5 mm. This shows the significance of making a mesh analysis and reducing the uncertainties of the modelling. But at the same time, a decrease of the SCFs values for the model meshed with finite element size of 1mm was pointed out. The corresponding model contained a huge number of finite elements and demanded a high computational time.

Table 3 depicted the SCFs values for the different finite element sizes. Also, the table shows that the SCFs values for the models with finite element sizes equal to 1 mm are lower compared to the other conditions. Therefore, this element size required a longer time to analyze.

Table 3. SCFs values for the different finite element size.

Finite element (mm)	SCF values
5	1.55
4	1.55
3	1.55
2	1.55
1	1.29

The SCFs obtained in the present analysis were compared with those by other authors who employed parametric equations under plane stress conditions. Hence, SCFs values estimated in this work were within the range of the data by those other authors, as shown in Table 4. The SCFs values reported by other authors varied from 1.38 to 1.71, and in the present analysis were around 1.29 (corresponding to elements of 1 mm). For higher elements, the SCF values were 1.55. In this study, a SCF value of 1.29 at the weld toe for a T-welded connection intact was considered. This value can be considered to be a low SCF value in T-welded connection. Dong [36], and Doerk [37] obtained a similar trend by performing finite element analysis of T-welded connections. In this case, an element size of 1 mm was used to mesh the load area. An element size of 2 mm was utilized to mesh the outer load area.

Table 4. Comparison of SCFs with other authors.

This work	Monahan [38]	Brennan [9]	Ida and Uemura [39]
1.29	1.45	1.38	1.71

Figure 8 shows finite element simulations of the T-welded connection both intact and with grinding. In this sense, it is noted that the higher stresses are situated along the weld toe, see Figure 8a). It can be observed that higher stresses, for the U-shaped condition, are found at the edge of the grinding (for a grinding depth of 10 mm), as shown in Figure 8b). Figures 8c) and 8d) show a stress state approach for the two grinding depths conditions of 6 mm and 10 mm, respectively. It is noted that the stress levels for the grinding depth of 10 mm are higher compared to the other grinding conditions since a higher amount of material was removed.

The SCFs were plotted on 2D and 3D graphs as seen in Figure 9a). In this sense, the complete section (grinding and intact area) was analyzed to indicate the stiffness contribution of all continuous plates. The SCFs for the three intact conditions, with a U-shape grinding depth of 6 mm and 10 mm are graphically represented in Figure 9b). It is pointed out that the stress increases as the depth increases. Also, the SCFs have a strong dependence on the geometric modification by the U-shape grinding and grinding depths performed. For that reason, high SCFs, at the edge of the grinding can be considered zones with high localized SCFs. A similar trend has been described by [22]. These regions correspond to stress concentration zones where localized cracking could be eliminated. It is well-known that initial cracking is assumed to start from nodes with maximum principal stresses at the weld toe [22]. In intact T-welded connections, cracking can initiate at the weld toe, since it acts as a stress riser. Indeed, for the U-shape grinding, cracking could initiate at the edge of the grinding and propagate through the weld toe and bottom of the grinding. Then, in order to verify this assumption, it is necessary to perform fatigue testing [32].

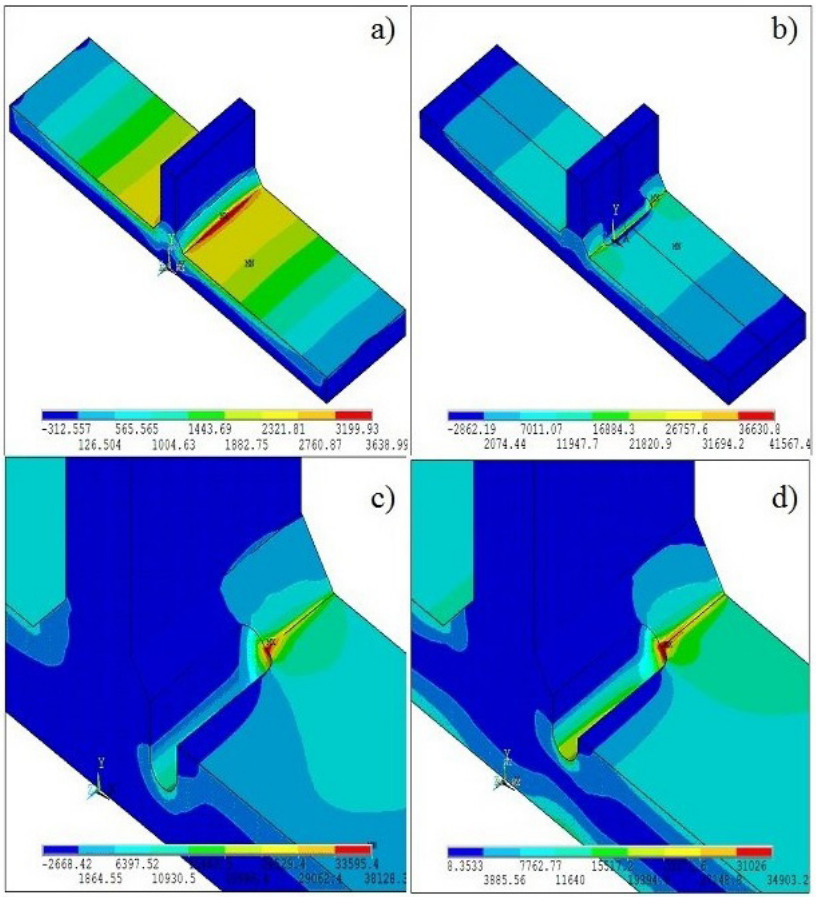

Figure 8. Principal stresses for T-welded connections. (a) intact; (b) U-shape grinding; (c) grinding depth of 10 mm; and (d) grinding depth of 6 mm.

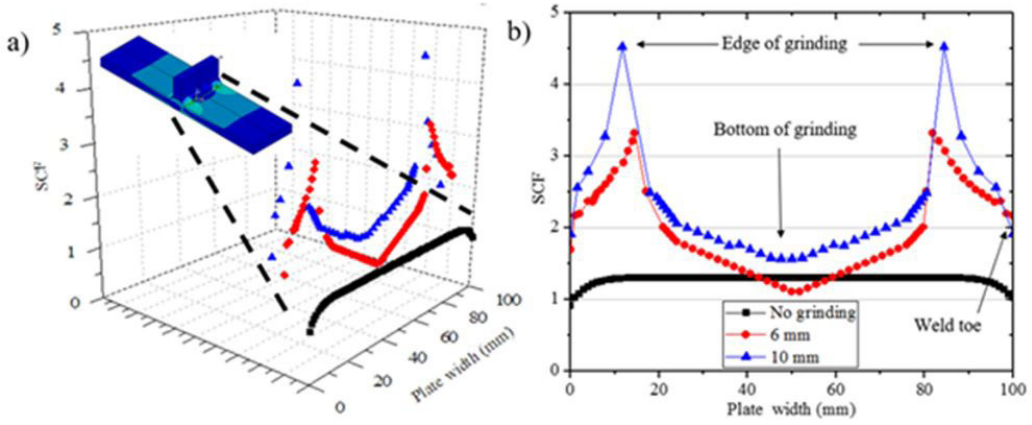

Figure 9. 3D and 2D plots of the SCFs for the T-welded connection. (a) complete T-welded connection; and (b) grinding conditions.

High stresses were achieved at the edge of the U-shape grinding. In this context, more analyses were conducted by smoothing the grinding edges at an angle of 135°, see Figure 10. It has been noticed that SCFs at the weld toe and in the grinding edges were smaller due to the smooth geometric transition region. The SCFs data obtained for different grinding conditions is presented in Table 5. It is observed that higher SCFs values are situated at the edge of the grinding. As the grinding depth increases, the SCFs at the weld toe, edge and bottom

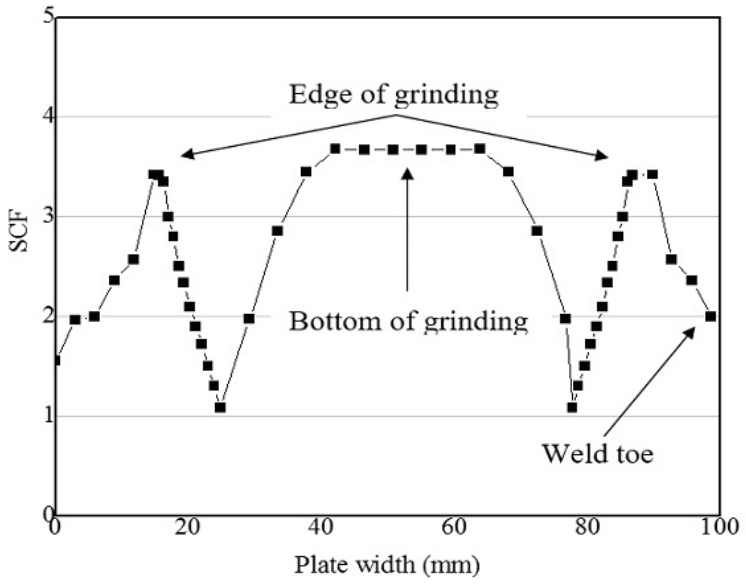

Figure 10. SCFs values for the T-welded connection with grinding smooth angle of 135° with a grinding depth of 10 mm.

Table 5. SCFs estimated for different regions of the U-shape grinding.

Condition	Grinding depth (mm)	SCFs		
		Weld toe	Edge of the grinding	Bottom of the grinding
Intact	No grinding	1.29	-	-
Grinding	6	1.68	3.31	1.1
	10	1.91	4.52	1.6
Grinding with smooth angle of 135°	10	1.55	3.3	3.67

increases. The structural integrity of the T-welded connections can be compromised due to the higher amount of material removed and high SCFs obtained.

3.2. Fatigue behavior of T-welded connections

All fatigue values are presented in Table 6. It was noted that, for the intact condition, the fatigue life is relatively high. Figure 11 presents the S-N curve tested for the T-welded connections under intact conditions. To adjust the dispersion of experimental results in one line point, regression analysis was applied. With stresses in the order of 317-344 MPa with cycles of 554,527-528,864, the connections did not fail. It is assumed that this value can be considered the fatigue limit in T-welded connections under intact conditions. A similar trend was established by other authors who used A36 steel [33], where a fatigue limit of 260 MPa is reported.

Table 7 shows the fatigue results for the T-welded connections with U-shape grindings at the weld toe for both grinding depths: 6 mm and 10 mm. Also, the table demonstrated that for the higher grinding depth, the cycle's number decreased in comparison with the intact condition. For a grinding depth of half of the plate thickness (10 mm), the fatigue life of the structure is reduced.

Figure 12 shows the S-N curves for the three conditions: intact, 6 mm and 10 mm of grinding depths and positions of the linear regression in the chart for the grinding conditions. In order to restore the fatigue life of the grinding connections, the position of the linear regression (for both grinding depths) would need to be close to the linear regression of the T-welded connections under intact conditions. The curves presented a reduced fatigue life

Table 6. Fatigue test results for intact T-welded connections.

No. of cycles	Applied stress MPa (ksi)
114083	675 (98)
116680	592 (86)
163829	572 (83)
153233	510 (74)
174645	482 (70)
385349	434 (63)
388204	365 (53)
528864	344 (50) Did not fail
554527	317 (46) Did not fail

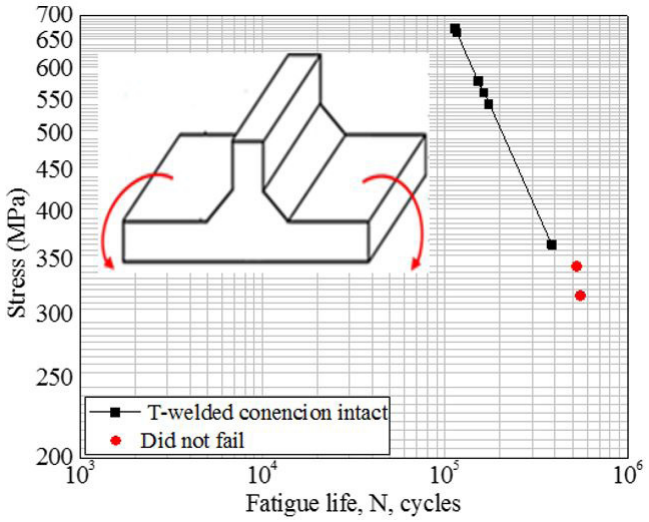

Figure 11. Classical S-N curve for estimating total life for intact T-welded connections under bending load.

Table 7. Fatigue results for T-welded connections with two grinding depths.

Load level	Cycles number	
MPa (ksi)	6 mm grinding depth	10 mm grinding depth
434 (63)	102179	39191
468 (68)	64155	28781
537 (78)	59789	22479
572 (83)	73158	23493

due to the repaired structures, especially for the grinding depth of 10 mm (50% of the plate thickness). To restore the fatigue life of the welded structures, the grinding depth should be as low as possible but at the same time it must remove cracking material.

Therefore, to observe the behavior of the SCFs on the S-N curves, such values were plotted in the S-N curves for the different grinding conditions, see Figure 13. As a continuation of the preceding section regarding SCFs obtained by finite element method, the results indicate an SCF value of 1.29 for T-welded connections without grinding. For SCFs values of 3.31 and 4.52 with grinding depths of 6 mm and 10 mm, respectively, the linear regression in the fatigue life decreased. For higher SCFs values, the fatigue life is considerably reduced. High SCF concentration in welded components occurs at weld discontinuities and is affected by weld geometry parameters such as weld toe radius, weld flank angles and weld throat [25]. Figure 13 associates the SCFs values in the S-N curves, and

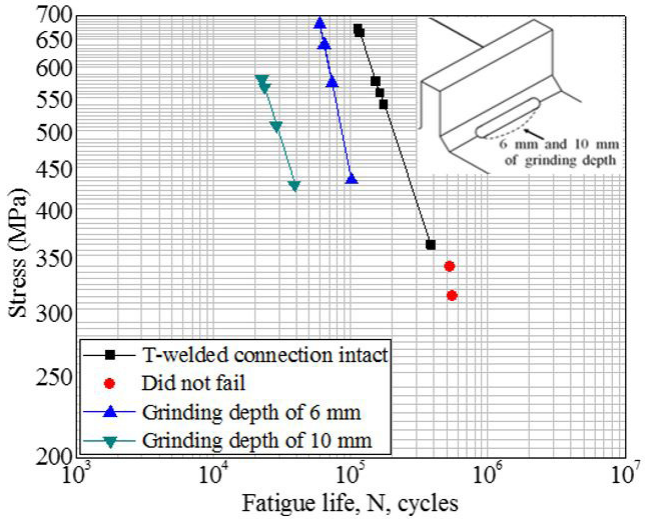

Figure 12. S-N data for T-welded connection with U-shape grinding depths of 6 mm and 10 mm.

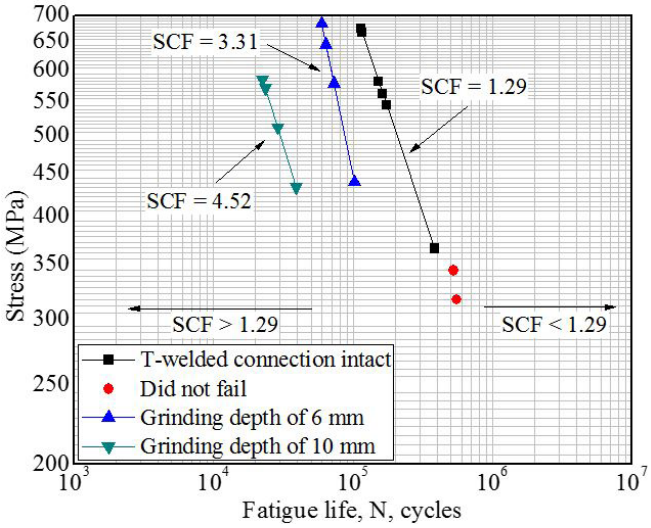

Figure 13. Correlation of the SCFs calculated by finite element in the S-N data of T-welded connection with intact and grinding conditions.

how the SCFs influence the fatigue behavior of the T-welded connections, but they do not influence the fatigue cycle´s number once a grinding condition is established. Then, the SCFs estimated can be used to establish a SCF threshold (equal to 1.29) to guarantee structural integrity of the T-welded connections with grinding depths. Also, the fatigue life obeys the S-N data for the welded structure under intact conditions. Consequently, it is expected that SCFs values of 1.29 correspond to the linear regression for the intact T-welded connections.

From an engineering point of view, this behavior was attributed to the following points: firstly, a great amount of material was eliminated in the U-shape grinding process. Therefore, it produces high SCFs values and reduces the fatigue life. During the welding process to construct T-welded connections, different types of material flaws and imperfections are induced in the welded joints. Material flaws, such as softening in the heat affected zone (HAZ) and residual stresses, have a great impact on the reduction of the fatigue life. The presence of weld imperfections, such as undercuts, cold laps and small toe radii increases the SCFs in the vicinity of the weld toe and, hence, decreases the fatigue life [24]. Secondly, high SCFs data was obtained, and is at the edge of the U-shape grinding. Several fatigue cracks emerged at the initial stage, at the edge of the U-shape grinding, and coalesced into a single crack that propagates at the weld toe [22]. Fatigue cracks were initiated at several points along the weld toe, and

coalesced into a large, semi-elliptical shape during crack propagation. In welded joints, crack initiation resulted in a location with an undercut and small toe radius, which could be expected since these imperfections increase the stress concentration in the weld toe [24]. In T-welded joints, fatigue cracking initiates at the weld toe, which acts as a raiser, and propagates through the main plate to the final fracture [25]. Maddox et al [40] found that failure under bending tests could fail at the weld toe or weld root. Then, as a consequence of high SCFs data, the linear regression for SCFs values of 3.31 and 4.52 were displaced to the left zone in Figure 13, producing a decrease in the fatigue life. Finally, the linear regression for high SCFs values decreased the fatigue life and could not restore the linear regression for SCF values of 1.29.

To increase the fatigue life in welded joints, several works are conducted. Maddox et al [40], used the weld toe radius of T-welded joints for bending fatigue loading configuration to deduce the SCFs. It is well known that the fatigue strength of most welded joint configurations could be improved by shot peening. An increased fatigue life is obtained, due to the low flank angle created during the welding of the second pass which reduces the stress concentration in the weld toe, prolonging the fatigue life [24]. Another option, tungsten inert gas, is employed. The main purpose of tungsten inert gas dressing is to remove weld toe flaws by re-melting the material at the weld toe and to reduce the local stress concentration effect of the local weld toe profile by providing a smooth transition between the plate and the weld face. Increasing the weld toe radius leads to lower SCFs values [25]. In the weld toes, there are peaks induced by the weld shape, e.g., by the weld toes [41].

The SCF values at the edge of the U-shape grinding should be carefully used and compared with the SCF values at the weld toe and of T-welded connections under intact conditions. It is due to the fact that they are singular points with high SCF values. Nowadays, some empirical formulas to estimate SCFs are available and will continue developing more works of SCFs for welding joints. It is due to the interest of SCFs in the fatigue life. However, ranges of application are not always clearly defined, nor are the hypotheses about their local geometry [41]. This relates SCFs data with S-N curves. The S-N curves still provide a reasonable estimate of initiation lives. However, in the present work, since a small number of scattered experimental data was tested, it could help to prevent evaluating linear regression for fitted S-N curves for intact T-welded connections and grinding depths.

4. Conclusions

Numerical methods such as the finite element analysis offer a precise calculation method for the estimation of SCFs for 3D T-welded connections under bending and loading. SCFs obtained by the finite element method indicate a SCFs value of 1.29 at the weld toe for T-welded connections without grinding. For T-welded connections with U-shape grinding and grinding depths of 6 mm and 10 mm, the SCF at the edge of the grinding were 3.31 and 4.52, respectively. In T-welded connections, the fatigue crack initiates at the weld toe, since it acts as a stress riser, and propagates through the weld toe until it produces the final fracture. In T-welded connections with U-shape grinding, a crack starts at the weld toe, and propagates towards the weld toe and bottom of the grinding. It is due to those zones that the weld toe and bottom of the grinding can present with high stresses.

In fatigue life assessment, it is very important to accurately determine the SCF. Defining the SCF, those can be correlated with the classical S-N curves. An SCF value of 1.29 was correlated with the S-N data of T-welded connections without grinding. For SCF values of 3.31 and 4.52, these values were in the left zone in the S-N curve for welded connections without grinding. For higher SCFs data, the fatigue life is considerably reduced. To improve or reinstall the original fatigue life, SCF at the U-shape grinding obtained must be low and close to 1.29. For T-welded connections without grinding, increasing the weld toe radius to lower SCF data is recommended. For T-welded connections with U-shape grinding, second pass welding can be applied to reduce SCF. However, during the welding process, different types of material flaws and imperfections are induced in the welded joints producing high SCF values and reducing the fatigue life.

Acknowledgements

The authors thank to Instituto Politécnico Nacional (ESIQIE-IPN), Instituto Mexicano del Petróleo (IMP), and CONACYT México, for the financial and material support.

References

[1] México. NRF-003-PEMEX: diseño y evaluación de plataforma marinas fijas en el golfo de México. México: Comité de Normalización de Petróleos Mexicanos y Organismos Subsidiarios; 2007.

[2] México NRF-175-PEMEX: acero estructural para plataformas marinas. México: Comité de Normalización de Petróleos Mexicanos y Organismos Subsidiarios; 2007.

[3] México. NRF-186-PEMEX: soldadura en acero estructural para plataformas marinas. México: Comité de Normalización de Petróleos Mexicanos y Organismos Subsidiarios; 2007.

[4] Terán G, Albiter A, Cuamatzi-Melendez R. Parametric evaluation of the stress concentration factors in T-butt welded connections. Engineering Structures. 2013;56:1484-1495. http://dx.doi.org/10.1016/j.engstruct.2013.06.031.

[5] Department of the Interior. MMS Project 642: assessment of damage and failure mechanisms for offshore structures and pipelines in Gustav and Ike. Final report. Houston: Energo Engineering; 2010 Feb.

[6] Haagensen PJ, Maddox SJ. IIW Recommendations on post weld improvement of steel and aluminum structures. The International Institute of Welding; 2001.

[7] Baik B, Yamada K, Ishikawa T. Fatigue crack propagation analysis for welded joints subjected to bending. International Journal of Fatigue. 2011;33(5):746-758. http://dx.doi.org/10.1016/j.ijfatigue.2010.12.002.

[8] Rodriguez-Sanchez JE. Brennan FP, Dover WD. Minimization of stress concentration factors in fatigue crack repairs. International Journal of Fatigue. 1988;20(10):719-725.

[9] Brennan FP, Peleties P, Hellier AK. Predicting weld toe stress concentrations factors for T and skewed T-joint plate connections. International Journal of Fatigue. 2000;22:573-584. http://dx.doi.org/10.1016/S0142-1123(00)00031-1.

[10] Rodriguez-Sanchez JE, Dover WD, Brennan FP. Application of short repairs for fatigue life extensión. International Journal of Fatigue. 2004;26(4):413-420. http://dx.doi.org/10.1016/j.ijfatigue.2003.07.002.

[11] Angeles-Herrera D. Gonzalez-Velazquez JL, Morales-Ramirez AJ. Fatigue Crack propagation in SAW seam welds of API 5L X42 steel pipe in the radial short direction. Journal of ASTM International. 2010;7(3):355-370.

[12] Angeles-Herrera D, González-Velázquez J, Morales-Ramírez AJ. Fracture-Toughness evaluation in submerged arc-welding seam welds in nonstandard curved SE(B) specimens in the short radial direction of API 5L steel pipe. Journal of Testing and Evaluation. 2012;40(6):1-4. http://dx.doi.org/10.1520/JTE103903.

[13] Remes H, Varsta P, Romanoff J. Continuum approach to fatigue crack initiation and propagation in welded joints. International Journal of Fatigue. 2012;40:16-26. http://dx.doi.org/10.1016/j.ijfatigue.2012.01.007.

[14] Ghanameh MF, Thevenet D, Zeghlou A. Stress concentration in offshore welded tubular joints subjected to combined load. Journal of Materials Science and Technology. 2004;20:35-37.

[15] Thandavamoorthy TS. Experimental and numerical investigations on unstiffened tubular T-joints of offshore platforms. Journal of Offshore Mechanical. 2009;131(4):041401.

[16] Mashiri FR, Zhao XL. Fatigue test and design of thin CHS-plate T-joints under cyclic in-plane bending. Thin Wall Structures. 2007;45(4):463-472. http://dx.doi.org/10.1016/j.tws.2007.03.002.

[17] Tso-Liang T, Chin-Ping F, Peng-Hsiang C. Effect of weld geometry and residual stresses on fatigue in butt-welded joints. International Journal of Pressure Vessels and Piping. 2002;79:476-482.

[18] Shao Y-B. Geometrical effect on the stress distribution along weld toe for tubular T-and K joints under axial load. Journal of Constructional Steel Research. 2007;63(10):1351-1360. http://dx.doi.org/10.1016/j.jcsr.2006.12.005.

[19] Mashiri FR, Zhao X-L. Thin circular hollow section-to-plate T-joints: Stress concentration factors and fatigue failure under in-plane bending. Thin-walled Structures. 2006;44(2):159-169.

[20] Cerit M, Kokumer O, Genel K. Stress concentration effects of undercut defect and reinforcement metal in butt welded joint. Engineering Failure Analysis. 2010;17(2):571-578. http://dx.doi.org/10.1016/j.engfailanal.2009.10.010.

[21] Rodriguez-Sanchez JE, Dover JE, Brennan FP. Design of crack removal profiles based on shape development of surface defects. Proceedings of the 22nd International Conference on Offshore Mechanics and Arctic Engineering; 2003 June 8-13; Cancún, México. Cancún: ASME; 2003. pp. 117-121. http://dx.doi.org/10.1115/OMAE2003-37198.

[22] Chen T, Xiao Z-G, Zhao X-L, Gu X-L. A boundary element analysis of fatigue crack growth for welded connections under bending. Engineering Fracture Mechanics. 2013;98:44-51. http://dx.doi.org/10.1016/j.engfracmech.2012.12.010.

[23] Sidhom N, Laamouri A, Fathallah R, Braham C, Lieurade HP. Fatigue strength improvement of 5083 H11 Al-alloy T-welded joints by shot peening: experimental characterization and predicitive approach. International Journal of Fatigue. 2005;27(7):729-745. http://dx.doi.org/10.1016/j.ijfatigue.2005.02.001.

[24] Holmstrand T, Mrdjanov N, Barsoum Z, Astrand E. Fatigue life assessment of improved joints welded with alternative welding techniques. Engineering Failure Analysis. 2014;42:10-21. http://dx.doi.org/10.1016/j.engfailanal.2014.03.012.

[25] Dabiri M, Ghafouri M, Raftar HRR, Björk T. Neural network-based assessment of the stres concentration factor in a T-welded joint. Journal of Constructional Steel Research. 2017;128:567-578. http://dx.doi.org/10.1016/j.jcsr.2016.09.024.

[26] Jen Y, Chang L, Fang C. Assessing the fatigue life of butt-welded joints under oblique loading by using local approaches. International Journal of Fatigue. 2008;30(4):603-613. http://dx.doi.org/10.1016/j.ijfatigue.2007.05.011.

[27] N'Diaye A, Hariri S, Pluvinage G, Azari Z. Stress concentration factor analysis for welded, notched tubular T-joints under combined axial, bending and dynamic loading. International Journal of Fatigue. 2009;31(2):367-377. http://dx.doi.org/10.1016/j.ijfatigue.2008.07.014.

[28] ANSYS. Introduction to ANSYS for release 14.5. Pensilvânia: ANSYS Inc.; 2015.

[29] Teran G, Cuamatzi-Melendez R, Albiter A, Maldonado C, Bracarense AQ. Characterization of the mechanical properties and structural integrity of T-welded connections repaired by grinding and wet welding. Materials Science and Engineering A. 2014;509:105-115. http://dx.doi.org/10.1016/j.msea.2014.01.078.

[30] Méndez GT, Cuamatzi-Meléndez R, Hernández AA. Combination of grinding and wet welding to repair localized cracking in T-welded connections. Materials Science Forum. 2014;793:51-58. http://dx.doi.org/10.4028/www.scientific.net/MSF.793.51.

[31] American Welding Society. D1.1/D1.1M:2006 structural welding code-steel. Florida: AWS; 2006.

[32] American Society for Testing and Materials. ASTM E 466: standard practice for controlled constant amplitude axial fatigue test of metallic materials. Pensilvânia: ASTM International; 1996.

[33] American Society for Testing and Materials. ASTM E468: standard practice for presentation of constant amplitude fatigue test results for metallic materials. Pensilvânia: ASTM International; 1990.

[34] Avila J, Franco F, Jaramillo H. Evaluación de la resistencia a la tensión y fatiga de uniones soldadas por fricción agitación de la aleación de magnesio AZ31b. Revista Latinoamericana de Metales y Materiales. 2012;32(1):71-78.

[35] Hobbacher AF. IIW recommendations for fatigue design of welded joints and componentes. Ohio: WRC; 2017. (Welding Research Council Bulletin, 520).

[36] Dong P. A structural stress definition and numerical implementation for fatigue analysis of welded joints. International Journal of Fatigue. 2001;23(10):865-876. http://dx.doi.org/10.1016/S0142-1123(01)00055-X.

[37] Doerk O, Frick W, Weissemborn C. Comparison of different calculation methods for structural stresses at welded joints. International Journal of Fatigue. 2003;25(5):359-369. http://dx.doi.org/10.1016/S0142-1123(02)00167-6.

[38] Monohan C. Early fatigue crack growth al welds. Southampton: Computational mechanics publications; 1995.

[39] Ida K, Uemura T. Stress concentrations factor formulas widely used in Japan. Fatigue & Fracture of Engineering Materials & Structures. 1996;19(6):779-786. http://dx.doi.org/10.1111/j.1460-2695.1996.tb01322.x.

[40] Maddox SJ. Fatigue if welded joints loaded in bending - supplementary report 84, Berkshire: TRRL; 1974.

[41] Pachoud AJ, Manso PA, Schleiss AJ. New parametric equations to estimate notch stress concentration factors at butt welded joints modeling the weld profile with splines. Engineering Failure Analysis. 2017;72:11-24. http://dx.doi.org/10.1016/j.engfailanal.2016.11.006.